Validation of downward surface radiation derived from MSG data by in-situ observations over the Atlantic ocean

ANDREAS MACKE[1], JOHN KALISCH[1] and RAINER HOLLMANN[2]

[1]Leibniz-Institut für Meereswissenschaften IFM-GEOMAR, Germany
[2]Deutscher Wetterdienst (DWD), Germany

(Manuscript received August 14, 2009; in revised form November 19, 2009; accepted March 3, 2010)

Abstract

The present work investigates the quality of the shortwave and and longwave downward radiation (DSR, DLR) at the sea surface over the Atlantic Ocean as retrieved from Meteosat Second Generation (MSG) measurements and EUMETSAT's Climate Monitoring - Satellite Application Facility (CM-SAF) algorithms. The observations taken at two transatlantic research cruises have been an ideal basis to be compared with the MSG products for DSR and DLR derived from Meteosat-8 and Meteosat-9. Onboard the research vessels "Akademik Ioffe" and "Polarstern" high quality in situ measurements of both radiation fluxes have been performed. Continuous full sky imagery and standard meteorological observations enable a comprehensive evaluation of the skills of MSG DSR- and DLR-retrievals in different climate zones and under various cloud and weather conditions. The DSR was retrieved by MSG with a positive bias of 2.77 Wm^{-2} during the Ioffe cruise, and 22.23 Wm^{-2} during the Polarstern cruise. The bias for the DLR was –1.73 Wm^{-2} and 2.76 Wm^{-2}, respectively. The differences between the two cruises mainly arise from the different weather conditions. No significant differences between the satellite products from Meteosat-8 and Meteosat-9 were found. In general DSR and DLR for clear sky conditions are captured with a high accuracy. Largest retrieval errors occur for fast fluctuating broken cloud conditions, though on average the MSG algorithm match the in-situ observations well. Semitransparent cirrus was found to cause a negative bias for the retrieved DSR. In tropics and subtropics the errors for DLR are smaller compared to higher latitudes. Most importantly, no significant dependencies of the satellite retrieval errors for both the DSR and the DLR on the solar elevation, near-surface humidity, cloud cover, SST and the shift of day and night were found, indicating that the CM-SAF radiation products are not subject to significant systematic errors.

Zusammenfassung

Diese Arbeit evaluiert die Qualität der abwärtsgerichteten kurzwelligen Einstrahlung (DSR) und der abwärtsgerichteten langwelligen Gegenstrahlung (DLR) an der Meeresoberfläche des Atlantischen Ozeans, berechnet aus Fernerkundungsdaten von Meteosat Second Generation (MSG) mit Hilfe der EUMETSAT Climate Monitoring – Satellite Application Facility (CM-SAF) – Algorithmen. Die auf zwei transatlantischen Forschungsfahrten gewonnenen Beobachtungsdaten stellen eine ideale Basis für den Vergleich mit den MSG-Produkten DSR und DLR dar, die aus Daten des Meteosat-8 und Meteosat-9 abgeleitet wurden. An Bord der Forschungsschiffe "Akademik Ioffe" und "Polarstern" wurden hochwertige in situ Messungen beider Strahlungsflüsse durchgeführt. Kontinuierliche Sequenzen der Wolkenkamera in Verbindung mit meteorologischen Standardmessungen ermöglichen diese Vergleichsstudie mit den Ergebnissen der MSG-Algorithmen für DSR und DLR in unterschiedlichen Klimazonen und unter verschiedensten Wolken- und Wetterbedingungen. Für die Fahrt der "Ioffe" zeigte die DSR abgeleitet aus MSG-Daten eine Überschätzung von 2.77 Wm^{-2}, für die Fahrt der "Polarstern" wurden 22.23 Wm^{-2} ermittelt. Der systematische Fehler der DLR war –1.73 Wm^{-2} bzw. 2.76 Wm^{-2}. Die unterschiedlichen Werte der beiden Fahrten resultieren hauptsächlich aus den verschiedenen Wetterbedingungen. Durch den zeitlichen Überlapp konnten Satellitenprodukte von Meteosat-8 und Meteosat-9 verglichen werden, die keine signifikanten Unterschiede zeigten. Im Allgemeinen werden DSR und DLR im wolkenfreien Fall mit hoher Genauigkeit wiedergegeben. Die größten Fehler im Algorithmus kommen bei sich schnell ändernder Cumulusbedeckung vor, wobei die berechneten Einstrahlungen im Mittel gut mit den in situ Messungen übereinstimmen. Semitransparenter Cirrus verursacht Unterschätzungen in der abgeleiteten DSR. In Tropen und Subtropen sind die Fehler in der DLR geringer als in hohen Breiten. Wichtig ist die Tatsache, dass der Fehler für den Satellitenalgorithmus sowohl für DSR als auch für DLR keine signifikanten Abhängigkeiten von dem Sonnenstand, von der Luftfeuchtigkeit in Bodennähe, vom Wolkenbedeckungsgrad, von der SST und vom Tag-Nacht-Unterschied zeigen. Dies weißt darauf hin, dass die CM-SAF Strahlungsprodukte keinen signifikanten systematischen Fehlern unterliegen.

*Corresponding author: Andreas Macke, Leibniz-Institut für Meereswissenschaften IFM-GEOMAR, Düsternbrooker Weg 20, 24105 Kiel, Germany, e-mail: macke@tropos.de

DOI 10.1127/0941-2948/2010/0433

0941-2948/2010/0433 $ 5.85

1 Introduction

The surface radiation budget that essentially drives our climate system most strongly affected by the presence of clouds. Satellite observations of the reflected solar and emitted thermal radiation at the top of the atmosphere (TOA) can be converted into the transmitted solar and re-emitted thermal radiation at the Earth's surface by means of scene identification and radiative transfer simulations. In the framework of EUMETSAT's "Climate Monitoring - Satellite Application Facilities" (CM-SAF; SCHULZ et al., 2009), remote sensing algorithms have been developed to provide DSR and DLR at the surface from MSG-SEVIRI and auxiliary informations (MUELLER et al., 2009). The accuracy of the satellite retrieval is limited by the number of independent observations and by inhomogeneities of the cloudy atmosphere within the satellite radiometers field of view (FOV). Thus, surface based observations of the state of the atmosphere and of the radiation budget are required to quantify the accuracy of the satellite retrievals. The Meridional Ocean Radiation Experiment (MORE) is a cooperative project of IFM-GEOMAR and the Shirshov Institute of Oceanology and was set up to conduct long-term high quality measurements of atmospheric parameters and surface fluxes in the Atlantic Ocean with a particular emphasis on clouds and radiation fluxes (SINITSYN et al., 2006; MACKE et al., 2007). In 2006 a research cruise between Germany and Uruguay on the Russian RV "Akademik Ioffe" has taken place and in 2007 the cruise on the German RV "Polarstern" (ANT XXIII-10) between Germany and South Africa has been performed (MACKE, 2008). The vessels cross all climate zones in several seasons, which provides an excellent opportunity for performing atmospheric measurements under a large variety of cloud, temperature and humidity conditions. The observations yield an unique basis for a validation study of CM-SAF's products of the downward shortwave and longwave radiation from Meteosat Second Generation data. The aim of this work is to estimate the errors and dependencies of the radiative MSG products. Previous work on this subject (MUELLER et al., 2009) has found an overall bias of –5 Wm^{-2} for DSR. The authors compared the satellite based fluxes with data from the baseline surface radiation network (BSRN; OHMURA et al., 1998) over Europe and Africa. Similar comparisons have been performed by HOLLMANN et al. (2006) over Europa and by BEHR et al. (2009) over ocean areas. HOLLMANN et al. (2006) report a bias of –7 Wm^{-2} for DSR and +15 Wm^{-2} for DLR on monthly mean time scale against measurements from BSRN measurements. BEHR et al. (2009) investigated the difference of CM-SAF products on a daily and monthly time scale with ship observations during a 19-month cruise through the Mediterranean Sea. They observed a bias of –8 Wm^{-2} for DSR and 8 Wm^{-2} for DLR, respectively. Their results are based on ship observations in the Mediterranean Sea and are limited to daily means, i.e. they exclude the effect of local illumination and atmospheric conditions on the error of the satellite retrieval. In the present work, the correlation of the retrieval error with latitude, solar elevation, total cloud cover, SST and the dependency on day and night time will be discussed. Due to the availability of high resolution full sky images a case-by-case study of the corresponding conditions of the cloudy skies will be performed.

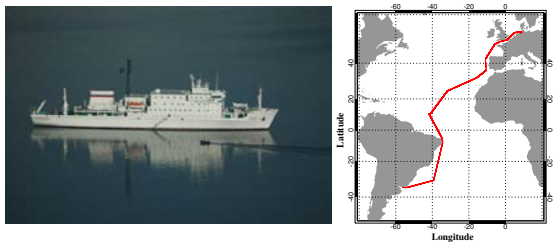

Figure 1: Russian Research Vessel *Akademik Ioffe* and the cruise track from Germany to Uruguay.

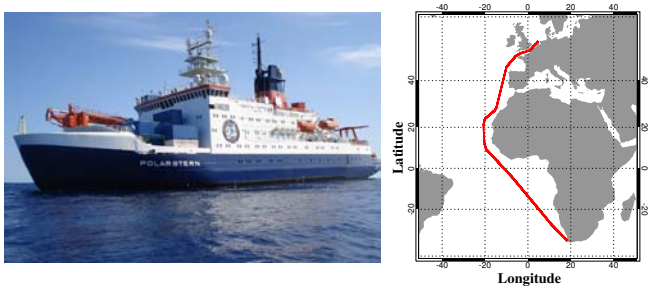

Figure 2: German Research Vessel *Polarstern* and the cruise track from South Africa to Germany.

2 MSG and CM-SAF radiation products

Within EUMETSAT's Satellite Application Facility on Climate Monitoring (CM-SAF) satellite data are used to derive climate parameters useful for climate monitoring studies in Europe and Africa. Today CM-SAF provides express products in high spatial and temporal resolution. The targeted variables are water vapor, cloud products as well as top of the atmosphere and surface radiation (SCHULZ et al., 2009). It is planned to release intercalibrated climate data sets for the mentioned climate variables. All CM-SAF products are available from www.cmsaf.eu.

The CM-SAF solar surface irradiance retrieval is based on radiative transfer calculations which uses satellite derived parameters as input.

The retrieval is applied to data from the Spinning Enhanced Visible and Infrared Imager (SEVIRI) and Geostationary Earth Radiation Budget (GERB) instruments

on-board the European operational weather satellite Meteosat Second Generation (MSG) and to Advanced Very High Resolution Radiometer (AVHRR) data on-board the National Oceanic and Atmospheric Administration (NOAA) and Meteorological Operational (MetOp) satellites for northern latitudes not covered by the geostationary satellite data. The retrieval relates top of atmosphere reflected radiation flux to the solar irradiance at the surface.

The CM-SAF algorithm MAGIC (Mesoscale Atmospheric Global Irradiance Code; MUELLER et al., 2009) is using two look-up tables (LUT) relating reflected spectral radiance to atmospheric properties, one for clear skies and one for cloudy skies.

The separate treatment of clear sky and cloudy sky situations is motivated by the fact that both situations are quite different with regard to the needed interpolation grid and the dominant physical processes. Inherent symmetries of the relation between the atmospheric state and transmission have been evaluated in order to define a basis system characterized by processes which can be treated as linearly independent on each other (MUELLER et al., 2009).

The LUTs contain the transmittance for a variety of atmospheric and surface states. Once the LUTs have been computed, the transmittance for a given atmospheric state can be extracted from the LUTs by interpolation for each satellite pixel and time. Finally, solar surface irradiance can be calculated from the transmittance by multiplication with the extraterrestrial incoming solar flux density.

In cloudy situations, the operational computation of the surface irradiance involves two steps. First the broadband TOA albedo is determined from the satellite measurement (e.g GERB, Geostationary Earth Radiation Budget). Then the atmospheric transmittance is determined from the pre-computed look-up tables using the TOA albedo together with information on the atmospheric state and surface albedo. For clear sky situations the transmittance is directly determined from the look-up tables.

To derive the longwave surface radiation (DLR) from satellite measurement an approach after GUPTA (1989) and GUPTA et al. (1992) have been used. From RTM model calculation they derived a regression which relates the cloudy and clear sky part of the downward longwave radiation. As input for this regression cloud coverage and cloud top height from satellite measurements are needed. In addition to this CM-SAF uses GME model data of integrated water vapor and the vertical profiles of temperature and humidity from GME (HOLLMANN et al., 2006).

3 Research cruises and measurements

The Russian research vessel *Akademik Ioffe* belongs to the fleet of the Shirshov Institute of Oceanology (Moscow). It was built for polar and oceanographic research, and is provided with an ice-strengthened hull.

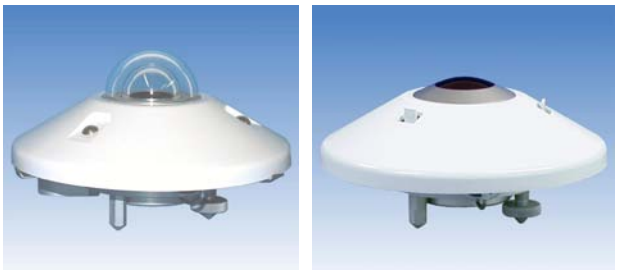

Figure 3: Pyranometer CM 21 (left) and Pyrgeometer CG 4 (right) manufactured by Kipp & Zonen.

On the cruise from Bremerhaven to Montevideo (Fig. 1) from October 12 until November 15, 2006 the following scientific devices have been used:

- pyranometer Kipp & Zonen CM 21
- pyrgeometer Kipp & Zonen CG 4
- net radiometer Kipp & Zonen CNR 1 for net radiation budget
- whole sky imager
- ships weather station for true windspeed, true wind direction, air temperature, relative humidity, air pressure.

The research ice breaker "Polarstern" is operated by the Alfred Wegener Institute for Polar and Marine Research (AWI). The construction type and properties were determined by the requirement to have a dual function both as a research and supply vessel in polar regions of the northern and southern hemisphere.

The transfer section ANT-XXIII/10 took place from Cape Town to Bremerhaven (Fig. 2) from April 12 until May 3, 2007. The following scientific device have been operated:

- ships onboard pyranometer Kipp & Zonen CM 21
- net radiometer Kipp & Zonen CNR 1
- microwave radiometer HATPRO
- periodical radio soundings Vaisala RS-92
- whole sky imager
- ships weather station (operated by the Deutscher Wetterdienst DWD) for true windspeed, true wind direction, air temperature, relative humidity, air pressure, sky and sea state classification

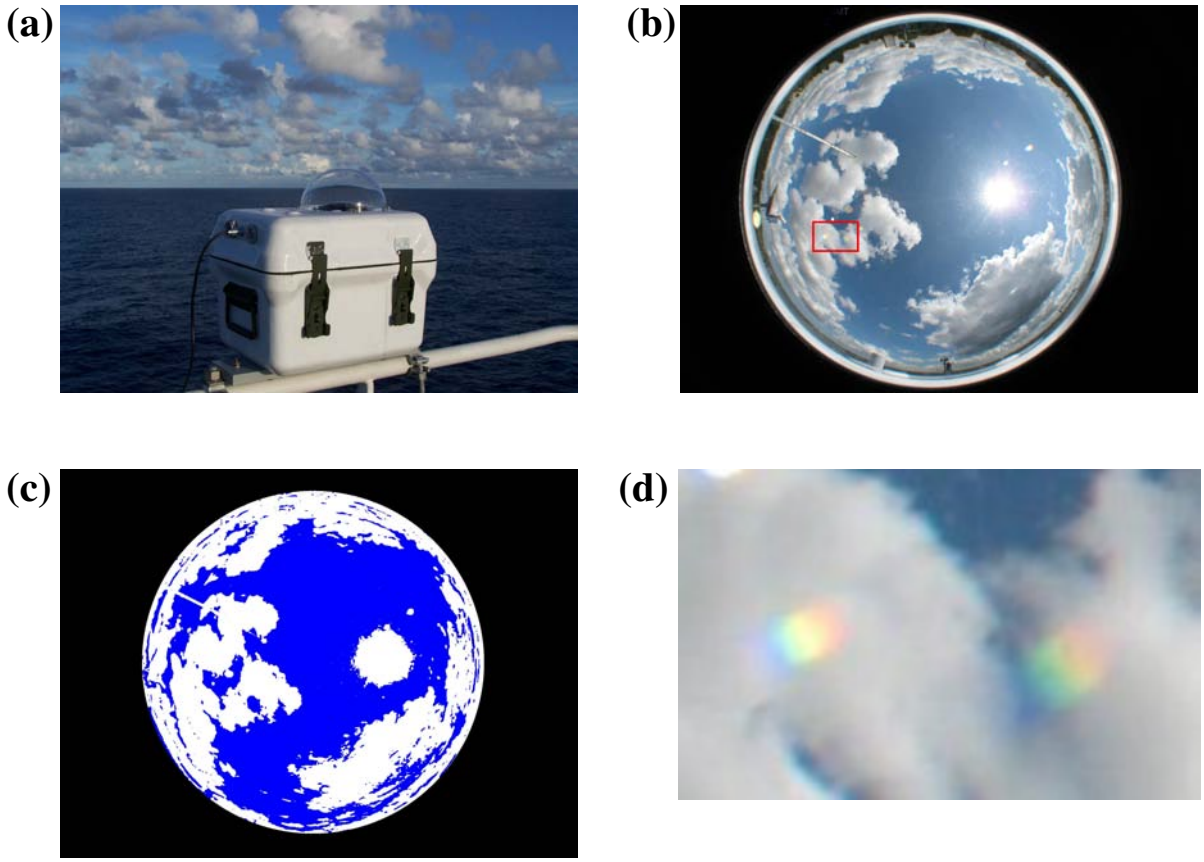

Figure 4: Full sky imager developed at IFM-GEOMAR (a) and its a field of view of 180° (b) with a red marked area of indicators of dispersion of direct sunlight. (c) displays the distribution of clouds and clear sky as calculated. The calculated total amount of clouds is $N = 0.39$. (d) shows a close-up view of red marked area in (b).

The Kipp & Zonen CM 21 (Fig. 3) pyranometer is a secondary standard pyranometer according to ISO 9060. The instrument covers the spectral range from 305 to 2800 nm with a response time (95 %) of 5 seconds. Kipp & Zonen expect maximal errors of 2 % for hourly sums and 2 % for daily sums of DSR (KIPP & ZONEN, 2004).

The pyrgeometer CG 4 (Fig. 3) is the appropriate instrument for measuring broadband longwave radiation fluxes. The spectral coverage is 4.5 to 45 μm with a response time (95 %) of 25 seconds. Due to solar heating of the instruments silicon window Kipp & Zonen expects maximal errors of $+4\,Wm^{-2}$ during an insolation of 1000 Wm^{-2}. For daily sums of DLR KIPP & ZONEN (2001) estimate an accuracy of 3 %.

The net radiometer CNR 1 consists of two pairs of up- and downward looking pyranometer and pyrgeometer. The instrument was used mainly as a standby radiometer. The present work only makes use of the DLR measurements. The spectral range of its pyrgeometer is from 4.5 to 42 μm with a response time (95 %) of 25 seconds. The radiation flux observations have been averaged over one minute which represents a compromise between capturing the sky conditions during the SEVIRI scan and to minimize errors due to specific ship orientations and due to slight deviations in recording time for the individual instruments (KALISCH and MACKE, 2008).

The full sky imager (Fig. 4a) is a low-cost device developed at the IFM-GEOMAR. It is based on commercially available standard components and is designed for rough offshore conditions on research vessels or platforms. Compared to other sky imagers (LONG et al., 2006) the IFM-GEOMAR imager operates without a direct sun shading by taking advantage of the latest technologies in digital cameras.

An example sky image is shown in Figure 4 (b). Figure 4 (c) displays the distribution of clouds and clear sky of the same image as calculated from the red versus blue threshold criteria given by LONG and DELUISI (1998). Errors occur whenever the direct sun is visible on the image. Pixels near the sun appear almost white and are miss-interpreted as cloudy. To correct for such errors direct sun situations have been identified from light dispersion of the formerly white direct solar beam on the acrylic glass dome (see Fig. 4 d). This method enables the full sky imager to record the direct sunshine (KALISCH and MACKE, 2008) on a moving ship, which is usually done by expensive pyrheliometer and pyra-

nometer systems on land stations only (HINSSEN and KNAPP, 2007).

From our human based cloud observations we find that 50 % of the images show a difference between the calculated and the observed total cloud cover of less than 10 %. This result coincides with the accuracy for camera based cloud covers given by FEISTER and SHIELDS (2005). Largest errors of up to 50 % occur during sunrise and sunset due to a enhanced scattering in the atmosphere and a change in the color composition of the images.

4 Comparison of MSG-products and ship-based measurements

The upward looking pyranometer is sensitive to the radiation field form the entire sky, with a stronger weight from the nadir. In order to optimize the comparison a first sensitivity study has been performed to find the MSG domain that fits best to the one-minute averaged pyranometer measurements. The following MSG-pixel averaging has been applied: single pixel, radius of 10km, 20km, and 40 km. A cosine-weighting procedure was used to provide the central pixel directly above the ship a maximum weight of 1, and zero-weight at the outer bound. The scanning of the Earth disc by SEVIRI takes 12 minutes (see SCHMETZ et al., 2002). This latitude dependent time delay has been taken into account when allocating MSG pixels to the ship position.

Fig. 5 shows the corresponding scatterplots between the MSG-pixel averaged shortwave radiant flux values and the one-minute time averages of the ship measurements. An optimal areal coverage with a maximum agreement is not directly obvious from the scatter plots. Table 1 lists bias, standard deviation, and correlation coefficient between ship and satellite based measurements for all combinations of research vessels, satellite, and size of areal averaging for both shortwave and longwave radiation.

In most cases for the DSR radiation either the single pixel satellite data or the 10 km average provides the smallest bias, smallest standard deviation, and largest correlation. Note that the single pixel and the 10 km averaged data show very similar results, indicating that cloud properties do not change much within this range. Also for the longwave radiation no significantly optimal resolution for the comparison could be identified.

For the remainder of this study both the single pixel value of MSG products and the cosine weighted 10 km average have been used. The latter roughly corresponds to the field of view of the ships instruments. Table 1 also reveals that the satellite retrieval tends to overestimate the DSR. While Meteosat-8 pixels directly above the ship on average overestimates the in-situ data during the Ioffe cruise data by 2.77 Wm^{-2} only, large mean positive biases of 14.26 Wm^{-2} for Meteosat-8 and 22.23 Wm^{-2} for Meteosat-9 are found for the Polarstern cruise. Using larger areas for averaging the Meteosat data even increases the overall differences.

A histogram (not shown here) of the differences between DSR from RV Polarstern and from the MSG products shows that a few but very large outliers with DSR(MSG) much larger than DSR(Polarstern) exist that are mostly responsible for the overall bias for Meteosat-8 and Meteosat-9 products. Visual inspection of the corresponding sky images reveals that local shadowing by small-scale clouds in a nearly cloud free sky and shadowing by the ships superstructure causes the much lower in-situ radiation values. If the 4 largest outliers are taken out of the analysis (less than 1.5 % of the data set), the average overestimations of the in-situ data are 7.33 Wm^{-2} for Meteosat-8 and 14.26 Wm^{-2} for Meteosat-9. Only during the Polarstern cruise, the radiometer mounted at the ships mast has been used in the analysis. Although mounted on a high and thus favorable position, the vicinity to the mast itself causes regular shadowing especially during low sun conditions.

We assume that the presence of undetected semitransparent cirrus clouds and aerosols leads to the general overestimation. In fact, a Sahara dust outbreak has been observed during the transect near the West African coast during the Polarstern cruise.

The Meteosat-8 based downward longwave radiation is negatively biased by 1.728 Wm^{-2} for the Ioffe cruise, and positively biased by 1.341 Wm^{-2} for the Polarstern cruise. The Meteosat-9 data yield a positive bias of 2.763 Wm^{-2}. Increasing the averaging area does not provide any significant changes. An underestimation by the satellite algorithm can either result from underestimating cloud amount or underestimating cloud bottom temperature. Again, undetected thin cirrus clouds which produce a temperature depletion work in the same direction. A rough estimate of cirrus frequencies based on the sky images revealed that 12 from 25 Ioffe cruise days reported cirrus clouds.

All comparisons as function of areal average (given as scatter plots in the same way than Fig. 5) between DSR and DLR measured on Polarstern and retrieved from Meteosat 8 and 9, respectively, were performed and analyzed (Table 1).

The cloud types for all radiation measurements have been identified by means of visual inspection of the sky imager data. Precipitation cases are still included in the ship data and are indicated as "precip" in the comparison plots. Situations with strong swell have not been excluded either, but rarely occurred during the ship cruises.

4.1 DSR case studies

Figure 6 shows an example case for the diurnal cycle of DSR from ship observations and from MSG for April 17, 2007. The day was dominated by Cu hum, which was only interrupted by a Cb during local noon. During this Cb event MSG captures the DSR and its variability

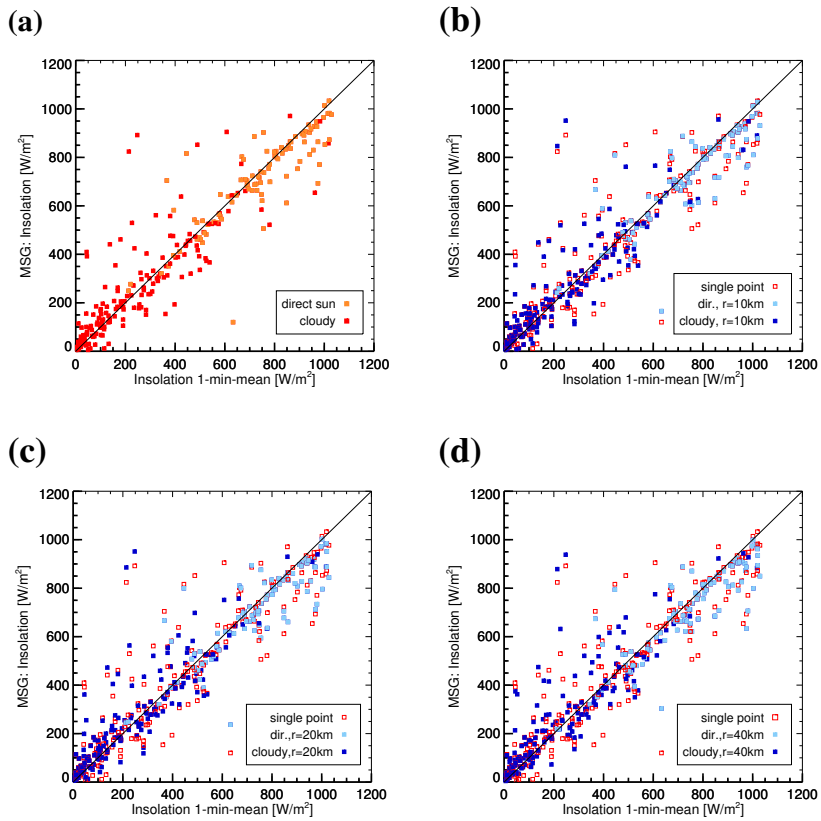

Figure 5: Scatterplot between Meteosat-8 shortwave dataset averaged for (a) the single point, (b) 10 km, (c) 20 km and (d) a radius of 40 km and the measurements on Ioffe.

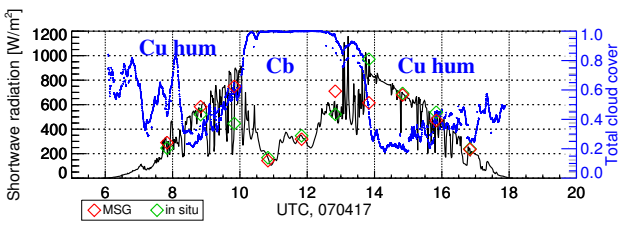

Figure 6: Downward shortwave radiation as measured and as retrieved by Meteosat-8, the total cloud cover calculated on full sky images and the synoptical observed clouds on April 17, 2007.

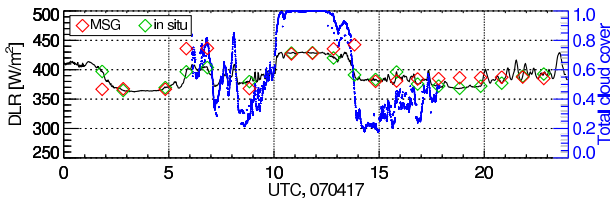

Figure 7: Downward longwave radiation on April 17, 2007.

surprisingly well, despite the fact that the reflected radiance should be nearly saturated at the large optical thickness that is characteristic for this cloud type. The completely overcast sky may have positively influenced the retrieval. On average, good agreements are also found for the broken Cu hum conditions.

It is obvious that large errors for the Meteosat products occur for fast fluctuating broken cloud conditions where MSG is not able to resolve the actual clouds structure due to its spatial and temporal resolution. Note that the observed DSR occasionally is larger than for clear sky conditions ("broken cloud effect"; SCHADE et al., 2007) for which the MSG algorithm is not trained. DSR under clear sky conditions is retrieved with high accuracy from MSG, whereas the presence of a semitransparent cirrostratus leads to an overestimation of insolation. Cumulonimbus with precipitation causes large positive and negative biases, even though the conditions did last for a few hours. In general, the bias under homogeneous stratiform cloud layers is small.

4.2 DLR case studies

Figure 7 shows an example case for the diurnal cycle of in situ and MSG-based DLR for the same day that has been discussed above for the DSR. As for the DSR the DLR is nicely captured even under the Cb cloud. Obviously, the MSG retrieval manages to estimate the cloud

Table 1: Bias $\overline{\Delta Q}$, standard deviation $stdev$, and correlation coefficient $corr$ between ship and satellite based measurements for all combinations of research vessel, satellite, and size of areal averaging.

Cruise on Ioffe, Meteosat 8						
	shortwave			**longwave**		
	$\overline{\Delta Q}$ $[W/m2]$	$stdev$ $[W/m2]$	$corr$	$\overline{\Delta Q}$ $[W/m2]$	$stdev$ $[W/m2]$	$corr$
single p.	2.77	114.9	0.933	-1.728	19.88	0.815
r=10km	3.08	107.4	0.941	-1.654	18.33	0.840
r=20km	4.74	108.7	0.940	-1.467	17.35	0.857
r=40km	6.05	110.8	0.937	-1.852	16.80	0.868
Cruise on Polarstern, Meteosat 8						
single p.	14.26	131.0	0.901	1.341	26.63	0.863
r=10km	20.67	127.4	0.905	2.160	24.11	0.882
r=20km	22.91	124.9	0.908	2.107	21.96	0.898
r=40km	24.10	126.3	0.905	2.176	20.86	0.904
Cruise on Polarstern, Meteosat 9						
single p.	22.23	121.3	0.925	2.763	27.39	0.848
r=10km	26.52	122.0	0.923	2.996	24.91	0.868
r=20km	27.25	120.9	0.924	2.642	22.75	0.886
r=40km	28.19	123.1	0.920	2.747	22.02	0.890

bottom temperatures quite accurately. There are two exceptions during the early morning which are caused by single clouds over the ship.

Occassionally, a continuous drift in the MSG DLR can be observed starting at sunset. Also jumps in the MSG DLR are seen, where no changes in cloud type and cloud cover have been observed. In general, DLR for clear sky conditions are captured quite accurately by MSG. For overcast conditions, biases occur in both directions.

5 Dependencies of retrieval errors on external factors

In the following, the MSG-retrieval errors will be discussed with respect to climatic conditions (described by the latitude), solar elevation, cloud cover, humidity, and sea surface temperature.

Figure 8 shows the DSR differences of MSG and in situ as a function of latitude for all cruises and for both MSG satellites. Both in absolute and in relative differences no significant latitudinal behavior can be detected.

There is an indication of larger DSR radiation differences (absolute and relative) at 10 degree north, which was caused by a local two-days ship station. The northern hemispheric relative differences are slightly smaller compared to the overall behavior. However, this might be due to a dominance of clear sky situations where the MSG retrieval works best.

Figures 9 and 10 show similar plots for the Polarstern cruise ANT-XXIII/10 and radiation flux retrieval results based on Meteosat-8 and Meteosat-9 data, respectively. For comparison, the data from Fig. 8 are also shown in red. Again, no significant latitudinal changes in the satellite based data are found. The same comparison for averaging the MSG pixel in an area with a radius of 10 km shows the same behavior as for the single pixel results discussed here.

The corresponding comparisons for the DLR are shown in Figs. 11, 12, and 13.

Note that the ordinate scale has been reduced compared to the shortwave cases. The differences in the longwave radiation are considerably smaller. Furthermore, because of the lack of a diurnal cycle in the longwave radiation, absolute and relative differences show nearly the same pattern. As for the DSR cases, no crucial latitudinal dependencies are found. However, in the tropical region between 5 degree south and 15 degree north the overall differences are slightly smaller with a negative bias in the MSG data. Again, the same comparison for averaging the MSG pixel in an area with a radius of 10 km shows the same behavior as for the single pixel results discussed here.

From this investigation of latitudinal dependencies of the MSG retrieval error we conclude that high cold clouds and large water vapor paths in the tropics, dry atmospheres with shallow convection in the subtropics and frontal clouds in midlatitudes have no specific effect on the performance of the MSG DSR algorithms. Furthermore, the overall biases between in situ and retrieved downward radiation fluxes at the sea surface appears to be very close to zero. The downward longwave radiation shows smaller errors compared to the DSR radiation. Except for a small negative bias in the tropics no significant latitudinal dependency is found as well.

Figure 14 shows the absolute and relative differences (with respect to Meteosat-8) in downward shortwave radiation as a function of solar elevation angle for the Ioffe cruise.

The differences are further separated into direct sun and shaded sun conditions (denoted as ”cloudy” in the

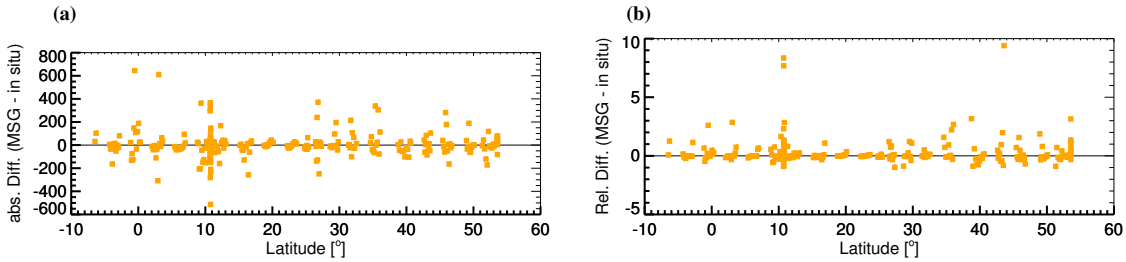

Figure 8: (a) Absolute [Wm^{-2}] and (b) relative [normalized] difference of shortwave radiation retrieved for the single pixel (Meteosat8) versus the latitude for the cruise on Ioffe.

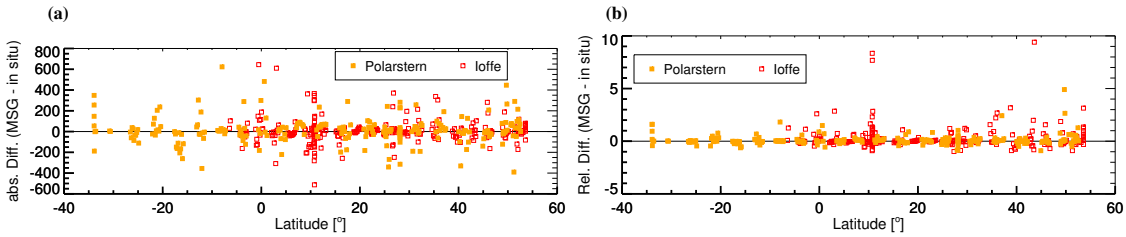

Figure 9: (a) Absolute [Wm^{-2}] and (b) relative [normalized] difference of shortwave radiation retrieved for the single pixel (Meteosat-8) versus the latitude for the cruise on Polarstern.

diagrams). The separation is based on the color spots on the camera images which only occur for direct illumination (see Fig. 4). Of course, absolute differences increase with increasing solar elevation. The differences are scattered almost symmetrically around the zero-bias line. The relative differences are largest near sunrise and sunset, where diffuse radiation at cloud sides and downward scattering from cloud bottoms prevail, which is not accounted for in the MSG algorithm[1]. Largest deviations of the MSG product are found at positive biases, i.e. at overestimation, and for shaded sun situations. This corresponds to individual Cu clouds that shade the radiometer onboard the ship, which cannot be resolved from the satellite data. Therefore, these errors are not of significance in judging the MSG performance. Relative differences for both direct sun and shaded sun conditions decrease with increasing solar elevation. Note that the ships rolling and pitching effects the radiation measurements stronger at low solar elevations, which may also cause some scatter in the relative differences.

The same analysis for the Polarstern cruise and DSR from Meteosat-8 is shown in Fig. 15. The overall dependency on solar elevation is similar both for the absolute and for the relative differences. Note that by construction Polarstern had less pitch and role, which might explain the reduced scatter at low solar elevation angles compared to Fig. 14. In contrast to the data from the Ioffe cruise, largest biases are found for direct sun situations, where the MSG product estimates considerably larger DSR than have been observed. A possible

[1]... which is also not required because of the small absolute values in this case

Table 2: Calculated correlation of solar elevation and the absolute and relative differences MSG minus measurements for all combinations of research vessel, satellite, and two sizes of areal averaging.

Ioffe/Meteosat-8, correlation of solar elevation with				
	shortwave		**longwave**	
	abs. diff.	**rel. diff.**	**abs. diff.**	**rel. diff**
single p.	-0.00317	0.10589	0.01547	0.01332
r=10km	-0.00621	0.12702	0.01651	0.01522
Polarstern/Meteosat-8, correlation of solar elevation with				
	abs. diff.	**rel. diff.**	**abs. diff.**	**rel. diff**
single p.	-0.11431	-0.01408	0.07821	0.06231
r=10km	-0.09724	0.04324	0.12553	0.10654
Polarstern/Meteosat-9, correlation of solar elevation with				
	abs. diff.	**rel. diff.**	**abs. diff.**	**rel. diff**
single p.	-0.14935	-0.01577	0.03262	0.01357
r=10km	-0.14614	0.01301	0.05814	0.03589

cause for this is cloud contamination in the SEVIRI field of view that is considered as overcast by the algorithm whereas direct sun still arrives at the surface.

This discrepancy can be further strengthend by enhanced downward scattering from clouds outside the solar disc (broken cloud effect). The synoptical overview of the Polarstern cruise (MACKE, 2008) indeed shows a dominance of shallow broken cloud situations in the southern and northern subtropics.

The correlation coefficients between solar elevation and the absolute and relative differences in downward shortwave and longwave radiation are summarized in Tab. 2 both for pixel based and 10 km average satellite

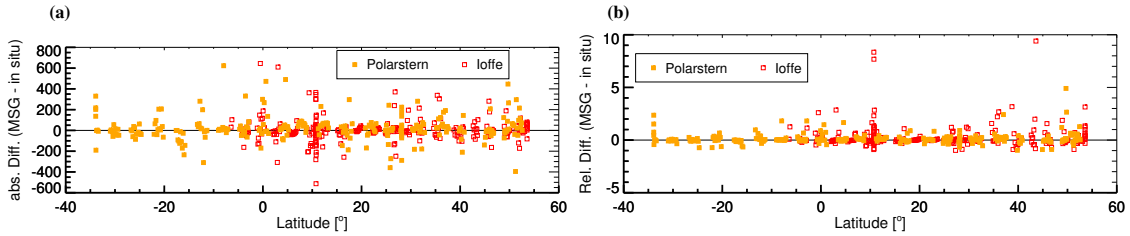

Figure 10: (a) Absolute [Wm^{-2}] and (b) relative [normalized] difference of shortwave radiation retrieved for the single pixel (Meteosat-9) versus the latitude for the cruise on Polarstern.

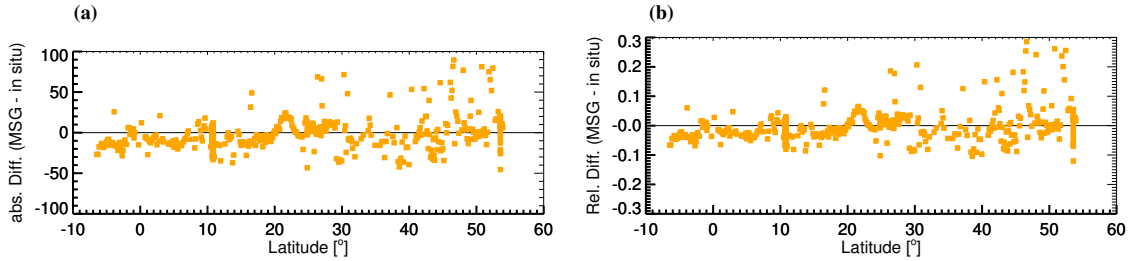

Figure 11: (a) Absolute [Wm^{-2}] and (b) relative [normalized] difference of longwave radiation retrieved for the single pixel (Meteosat-8) versus the latitude for the cruise on Ioffe.

products. For all combinations no significant (based on Student t-test) correlations were found. This implies that solar elevation has no systematic effect on the accuracy of the MSG-based DSR and DLR.

The dependency of absolute and relative shortwave differences for direct sun and for shaded sun cases on cloud cover as derived from the sky imager is shown in Fig. 16.

Smallest absolute errors occur for zero- or very low cloud cover due to MSGs high accuracy for clear sky conditions (see section 4.1). Largest errors are found for medium cloud cover, because of the higher occurrence of small scale sub-pixel clouds. For overcast conditions there is a large number of cases with an absolute difference close to zero, which coincides with the small errors found for stratus clouds. Shaded sun situations (denoted as "cloudy" in the diagram) show the largest differences, whenever the ship is shaded by a local cloud, which is not resolved by the satellite.

Table 3 lists the calculated correlation coefficients between the total cloud cover and the absolute and relative differences between DSR from satellite and ship measurements. An overall dependency of the DSR differences on cloud cover can not be identified.

Both DSR and DLR are affected by the amount of water vapor in the atmospheric column. Figures 17 and 18 show the MSG retrieval errors as a function of near-surface relative humidity for the shortwave and for the longwave radiation, respectively. We have made use of the near-surface humidity as it is strongly correlated with the column integrated water vapor. No correlation is found in both cases. Table 4 shows the calculated correlation coefficients between the humidity and the absolute and relative differences of radiation and measured flux. Thus, the retrieval errors do not exhibit a systematic dependency on near-surface humidity. The column water vapor was not under investigation.

Table 3: Calculated correlation of the total cloud cover and the absolute and relative differences MSG minus measurements for DSR.

Ioffe/Meteosat-8, correlation of cloud cover with		
	abs. diff.	**rel. diff.**
single point	0.0516	0.1923
r=10km	0.0836	0.2131

Table 4: Calculated correlation of humidity and the absolute and relative differences MSG minus measurements for two sizes of areal averaging.

Ioffe/Meteosat-8, correlation of humidity with				
	shortwave		**longwave**	
	abs. diff.	**rel. diff.**	**abs. diff.**	**rel. diff**
single p.	0.0785	0.2264	0.04102	0.0480
r=10km	0.0960	0.2374	0.0722	0.0830

The amount of upwelling thermal radiation that is subject to re-emission by atmospheric gases or backscattering by cloud particles is determined by the sea surface temperature. Therefore, DLR differences between in situ measurements and satellite retrieval are shown in Figs. 19 and 20 for the Polarstern cruise, and for Meteosat-8 and Meteosat-9, respectively.

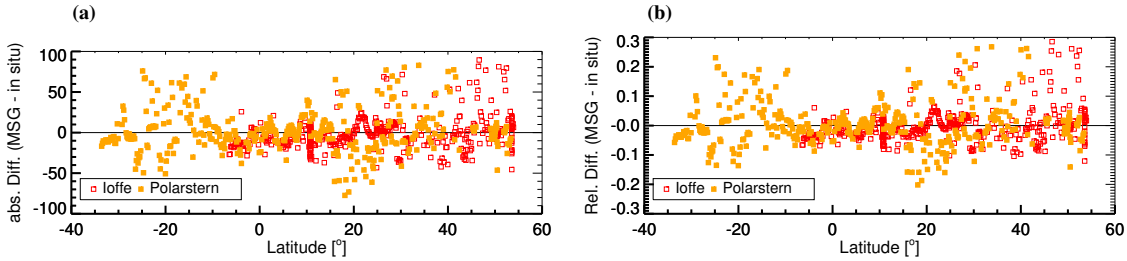

Figure 12: (a) Absolute [Wm^{-2}] and (b) relative [normalized] difference of longwave radiation retrieved for the single pixel (Meteosat-8) versus the latitude for the cruise on Polarstern.

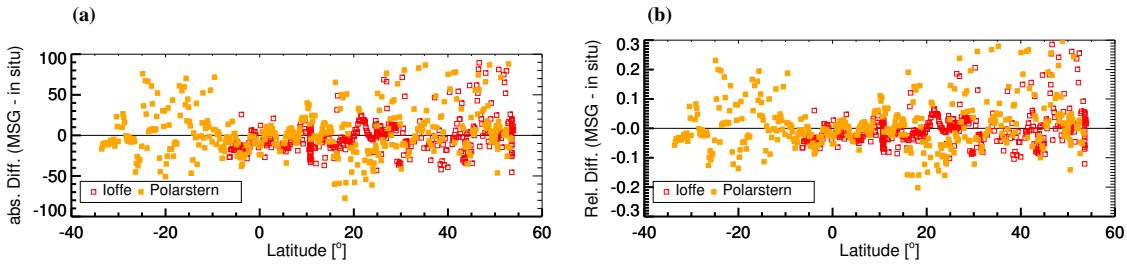

Figure 13: (a) Absolute [Wm^{-2}] and (b) relative [normalized] difference of longwave radiation retrieved for the single pixel (Meteosat-9) versus the latitude for the cruise on Polarstern.

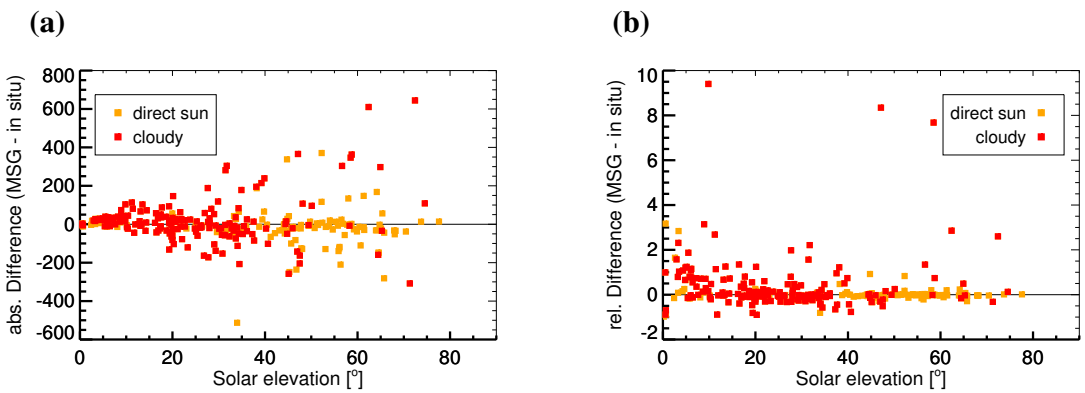

Figure 14: (a) Absolute [Wm^{-2}] and (b) relative [normalized] difference of shortwave radiation retrieved for the single pixel (Meteosat-8) versus the solar elevation for the cruise on Ioffe.

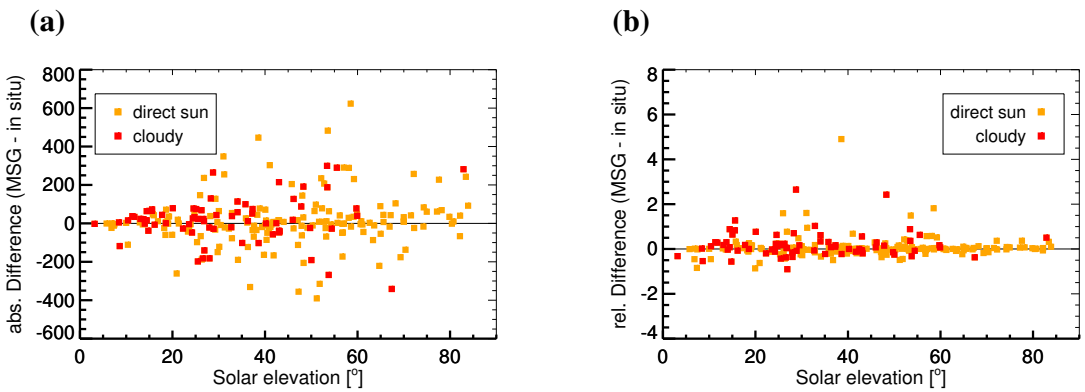

Figure 15: (a) Absolute [Wm^{-2}] and (b) relative [normalized] difference of shortwave radiation retrieved for the single pixel (Meteosat-8) versus the solar elevation for the cruise on Polarstern.

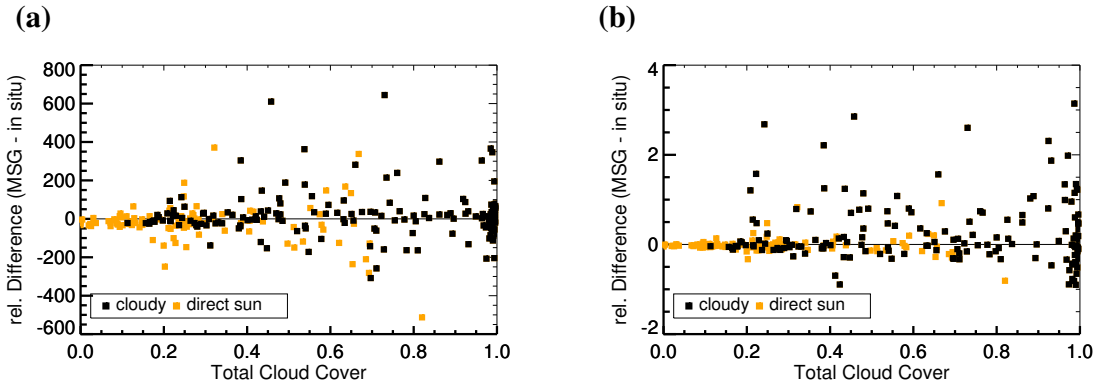

Figure 16: (a) absolute [Wm^{-2}] and (b) relative [normalized] difference of shortwave radiation retrieved for the single pixel versus the total cloud cover for the cruise on Ioffe (Meteosat-8).

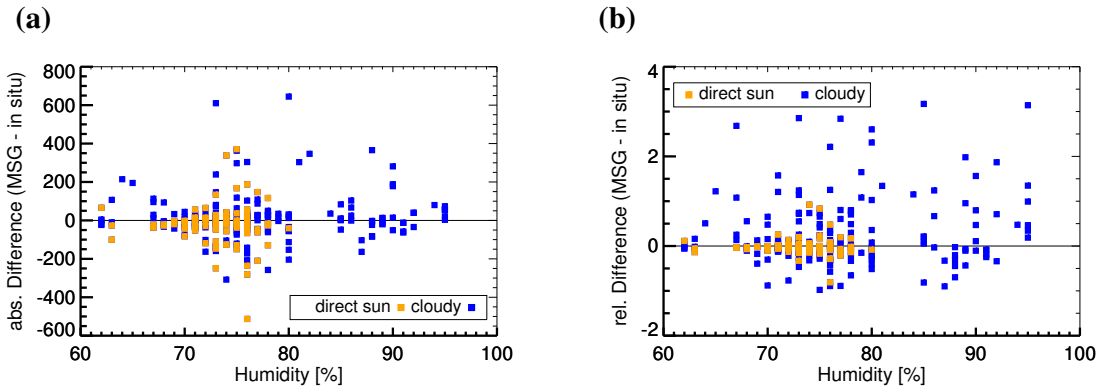

Figure 17: (a) Absolute [Wm^{-2}] and (b) relative [normalized] difference of shortwave radiation retrieved for the single pixel (Meteosat-8) versus the relative humidity for the cruise on Ioffe.

Small errors are found at the largest SST values. Those regions are located at the Inter-Tropical Convergence Zone (ITCZ), where strong convection might produce high reaching cold clouds tops that are well detected by the satellite. Also at small SSTs the errors are small, potentially due to fewer clouds at cold SSTs during this particular cruise. Indeed, visual inspection of the sky imager data do show a higher occurance of clear days with cold water temperatures, mostly driven by the specific synoptical situations.

6 Summary and conclusions

The present study investigates the quality of the downward shortwave and longwave radiation retrieved by MSG (Meteosat-8 and Meteosat-9) algorithms of the CM-SAF over the Atlantic ocean. The basis for this evaluation have been datasets of two transatlantic research cruises onboard the research vessels Ioffe and Polarstern. The DSR was retrieved by MSG with a positive bias of 2.77 Wm^{-2} during the Ioffe cruise, and 22.23 Wm^{-2} during the Polarstern cruise. The bias for the DLR was –1.73 Wm^{-2} and 2.76 Wm^{-2}, respectively. The differences between the two cruises mainly arise from the different weather conditions. No significant differences between the satellite products from Meteosat-8 and Meteosat-9 were found.

Largest errors occur for retrieved insolation of fast fluctuating broken cloud conditions, though on average the MSG-based data matches the in-situ observations well. Semitransparent cirrus was found to cause a negative bias for the retrieved DSR.

In tropics and subtropics the errors for DLR are reduced compared to higher latitudes. This might be due to the higher resolution of SEVIRI for nadir measurements or the dominating atmospheric conditions.

No significant dependencies of the satellite retrieval errors for both the DSR and the DLR on the solar elevation, near-surface humidity, cloud cover, SST and the shift of day and night were found for two research cruises. This indicates that the CM-SAF radiation products are not subject to significant systematic errors.

It appears surprising that the satellite retrieval, which are based on rather simplified plane parallel homogeneous cloud scenarios with constant cloud microphysical properties provides an overall good description of the in-situ radiation fluxes at the surface. ”One reason for

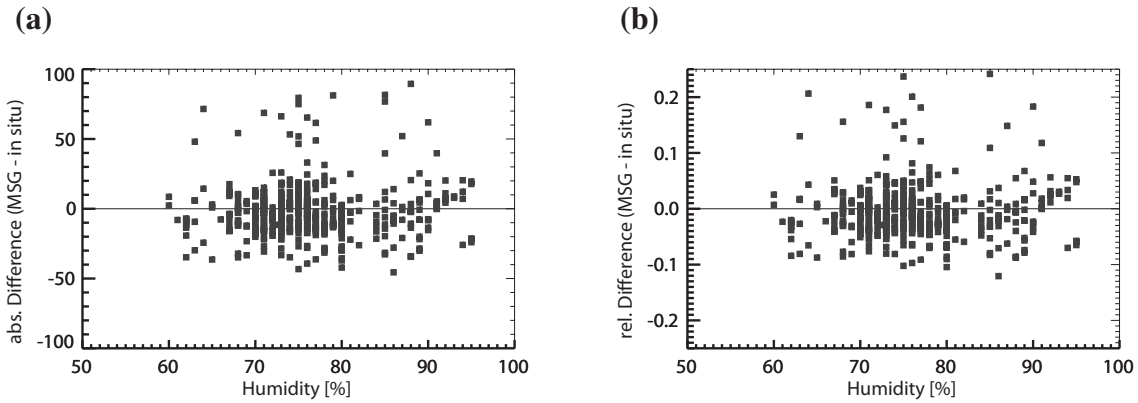

Figure 18: (a) Absolute [Wm^{-2}] and (b) relative [normalized] difference of longwave radiation retrieved for the single pixel (Meteosat-8) versus the relative humidity for the cruise on Ioffe.

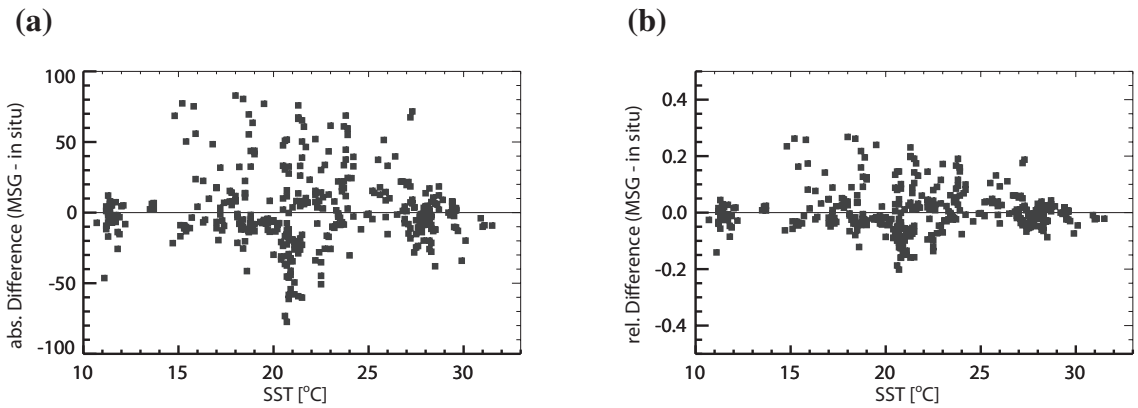

Figure 19: (a) Absolute [Wm^{-2}] and (b) relative [normalized] difference of incoming longwave radiation retrieved for the single pixel (Meteosat-8) versus the SST for the cruise on Polarstern.

the good agreement might result from compensation of errors in the cloud retrieval and in the radiative flux calculations. For example, underestimating cloud optical thickness due to the more reflective plane parallel homogeneous model clouds (compared to radiance-equivalent real 3d clouds) partly balances the higher transmissivity of the real 3d clouds (compared to optical thickness equivalent real 3d clouds).

Thus, it will also be an interesting task in the future to compare CM-SAF cloud products like liquid water path with corresponding observations from the ground.

Acknowledgments

This study was partly funded by Germany's National Meteorological Service, the Deutscher Wetterdienst (DWD), under working contract "OCEAN 2007".

We like to thank the Shirshov-Institute for Oceanology in Moscow and the Alfred-Wegener Institute for Polar and Ocean Sciences for enabling the participation on the Atlantic transects of the research vessels Academic Ioffe (fall cruise 2006) and Polarstern (ANT-XXIII/10). We acknowledge the excellent support from both ship crews.

References

BEHR, H.D., R. HOLLMANN, R.W. MUELLER, 2009: Surface radiation at sea: Validation of satellite-derived data with shipboard measurements. – Meteorol. Z. **18**, 61–74.

FEISTER, U., J.SHIELDS, 2005: Cloud and radiance measurements with the VIS/NIR Daylight Whole Sky Imager at Lindenberg (Germany). – Meteorl. Z. **14**, 627–639.

GUPTA, S., 1989: A parameterization for longwave surface radiation from sun-synchronous satellite data. – J. Climate **2**, 302–315.

GUPTA, S., W.L. DARNELL, A.C. WILBER, 1992: A parameterization for longwave surface radiation from satellite data: Recent improvements. – J. Appl. Meteor. **31**, 1361–1367.

HINSSEN, Y.B.L., W.H. KNAPP, 2007: Comparison of pyranometric and pyrheliometric methods for the determination of sunshine duration. – J. Atmos. Ocean. Technol. **24**, 835–846.

HOLLMANN, R., R.W. MUELLER, A. GRATZKI, 2006: CM-SAF surface radiation budget: First results with AVHRR data. – Adv. Space Res. **37**, 2166–2171.

KALISCH, J., A. MACKE, 2008: Estimation of the total cloud cover with high temporal resolution and parametrization of short-term fluctuations of sea surface insolation. – Meteorol. Z. **17**, 603–611.

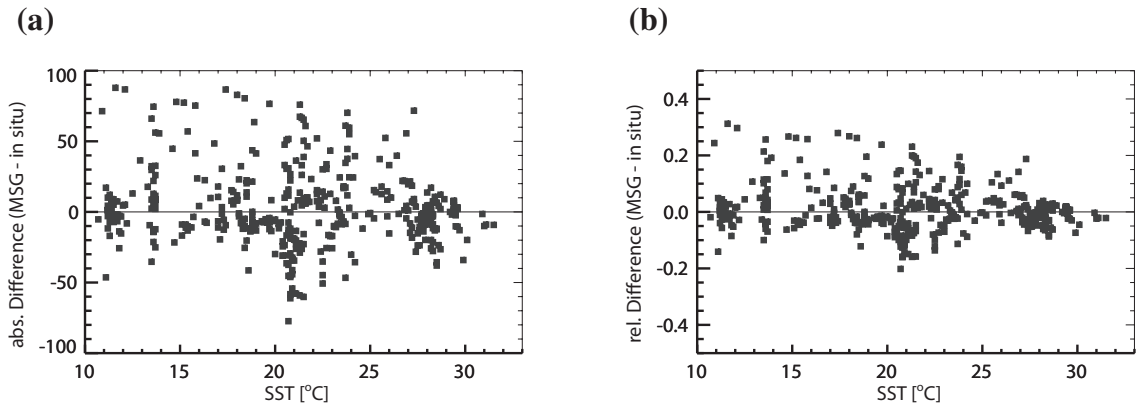

Figure 20: (a) Absolute [Wm^{-2}] and (b) relative [normalized] difference of incoming longwave radiation retrieved for the single pixel (Meteosat-9) versus the SST for the cruise on Polarstern.

KIPP & ZONEN, 2001: Instruction Manual CG 4. – Manual Version: 0304, www.kippzonen.com/download/kipp_manual_cg4_1324.pdf, 20.06.2008.

KIPP & ZONEN, 2004: Instruction Manual CM 21. – Manual Version: 0904, www.kippzonen.com/download/kipp_manual_cm21_1410.pdf, 05.03.2008.

LONG, C.N., J.J. DELUISI, 1998: Development of an Automated Hemispheric Sky Imager for Cloud Fraction Retrievels. – In: 10th Symp. on Meteorological Observations and Instrumentation January 11 to 16, 1998, Phoenix, AZ.

LONG, C.N., J.M. SABBURG, J. CALBÓ, D. PAGÈS, 2006: Retrieving cloud characteristics from ground-based color all-sky images. – J. Atmos. Ocean. Technol. **23**, 633–652.

MACKE, A., 2008: The expedition ANTARKTIS-XXIII/10 of the research vessel "Polarstern" in 2007 / Ed. by Andreas Macke. – In: Berichte zur Polar- und Meeresforschung – Reports on polar and marine research **575**, 37 pp.

MACKE, A., J. KALISCH, A. SINITSYN, A. WASSMANN, 2007: More of MORE: the first MORE cruise onboard RV Polarstern. – Flux news **4**, 21–22.

MUELLER, R.W., C. MATSOUKAS, A. GRATZKI, H.D. BEHR, R. HOLLMANN, 2009: The CM-SAF operational scheme for the satellite based retrieval of solar surface irradiance: A LUT based hybrid Eigenvector approach. – Rem. Sens. Env. **113**, 1012–1024.

OHMURA, A., E. DUTTON, B. FORGAN, 1998: Baseline surface radiation network (BSRN/WCRP): new precision radiometry for climate research. – Bull. Amer. Meteor. Soc. **79**, 2115–2136.

SCHADE, N.H., A. MACKE, H. SANDMANN, C. STICK, 2007: Enhanced solar global irradiance during cloudy sky conditions. – Meteorol. Z. **16**, 295–303.

SCHMETZ, J., P. PILI, S. TJEMKES, D. JUST, J. KERKMANN, S. ROTA, A. RATIER, 2002: An introduction to meteosat second generation (MSG). – Bull. Amer. Meteor. Soc. **83**, 977–992.

SCHULZ, J., P. ALBERT, H.-D. BEHR, D. CAPRION, H. DENEKE, S. DEWITTE, B. DURR, P. FUCHS, A. GRATZKI, P. HECHLER, R. HOLLMANN, S. JOHNSTON, K.G. KARLSSON, T. MANNINEN, R.W. MUELLER, M. REUTER, A. RIIHELA, R. ROEBELING, N. SELBACH, A. TETZLAFF, W. THOMAS, M. WERSCHECK, E. WOLTERS, A. ZELENKA, 2009: Operational climate monitoring from space: the EUMETSAT satellite application facility on climate monitoring (CM-SAF). – Atmos. Chem. Phys. **9**, 1687–1709.

SINITSYN, A., S. GULEV, A. MACKE, J. KALISCH, S. SOKOV, 2006: MORE cruises launched. – Flux news **1**, 11–13.